PHYSICAL REVIEW B **91**, 121411(R) (2015)

Giant nonlinear magneto-optical response of magnetoplasmonic crystals

V. L. Krutyanskiy,[1] A. L. Chekhov,[1] V. A. Ketsko,[2] A. I. Stognij,[3] and T. V. Murzina[1]
[1]*Department of Physics, Moscow State University, Moscow 119991, Russia*
[2]*Kurnakov Institute of General and Inorganic Chemistry, RAS, Leninsky Prospect 31, Moscow 119991, Russia*
[3]*Scientific-Practical Materials Research Centre of NAS of Belarus, P. Brovki Street, Minsk 220072, Belarus*
(Received 10 December 2014; revised manuscript received 28 February 2015; published 24 March 2015)

Magnetoplasmonics provides unique possibilities for magnetic field control over light flow. A special interest in this field is attracted to magnetoplasmonic crystals (MPCs) that are nanostructured metal-dielectric materials with rich resonant spectra that can be tuned by a magnetic field. We show that MPC demonstrates enhanced nonlinear-optical effects such as optical second harmonic generation (SHG) and a giant nonlinear magneto-optical effect. Contrary to the linear-optical case, the main mechanism underlying the observed effects is the resonant enhancement of the local field achieved both for the surface-plasmon-polariton modes at metal/dielectric interfaces and for the waveguide modes in a dielectric slab, which provides an up to 25% magnetic field controlled SHG intensity variation. These effects are treated as an interplay of excitation of different modes that leads to Fano-type resonances in the nonlinear-optical response.

DOI: 10.1103/PhysRevB.91.121411 PACS number(s): 42.65.−k, 73.20.Mf, 78.20.Ls, 79.60.Jv

Magnetoplasmonic crystals (MPCs) are spatially periodic nanostructures combining the features of surface-plasmon-polariton (SPP) excitation and magneto-optical tunability. It is highly possible that these structures may be used for magnetic field control over light flow. Coupled localized states of light and electrons at the metal-dielectric interface that are the surface plasmon polaritons can be excited at a metal-dielectric interface and thus introduce resonant MPC features and strong localization of the optical field in a thin interface layer. One of the promising MPC compositions contains a low-loss magnetic dielectric slab covered by a thin perforated metal layer. In such a structure, surface plasmon polaritons are exited through light diffraction on the metal grating, while the excitation conditions can be modulated by magnetization of the dielectric layer. A number of experimental works have shown the MPC operation performance to be of high quality [1–6]. Moreover, under a proper design, MPCs can also support resonant excitation of waveguide modes (WGs) that may be tuned by the magnetic field as well [1,4,7].

Since the excitation of resonant modes can significantly enhance local optical fields, the induced nonlinear-optical processes should reveal specific spectral features. In particular, plasmon-enhanced Raman scattering [8] and optical second harmonic generation (SHG) enhanced by SPP excitations were studied [9,10]. The well-recognized surface [11] and magnetization [12] SHG selectivity makes it an extraordinarily sensitive technique for studies of all types of resonant MPC modes. This was demonstrated for a number of structures, such as a uniform ultrathin magnetic layer placed between noble metal layers, nickel gratings, perforated Co layers, etc. [13–16].

In this Rapid Communication we present a study on magnetization control over the intensity and phase of optical second harmonic generation in one-dimensional (1D) garnet-based MPCs. We provide an experimental evidence of a strong modulation of the SHG intensity and of the nonlinear magneto-optical MPC response induced by SPP and waveguide modes. In particular, SHG phase measurements reveal a drastic phase modulation of a plasmon-assisted second harmonic wave close to the resonant SPP excitation.

Figure 1 shows a schematic view of the studied MPC structure, along with the experimental geometry. The MPC consists of a 2 μm thick bismuth iron garnet (BIG) layer grown on a gadolinium gallium garnet (GGG) substrate and covered by a 40 nm thick perforated gold film that forms a grating with a period of $d = 730$ nm, as is shown on the scanning electron microscopy (SEM) image in the inset of Fig. 1. The sample was made using a recently developed method of combined ion-beam etching [17,18]. The excitation of two types of optical modes, namely, the SPP at two metal surfaces and waveguide modes in the magnetodielectric slab, is expected in such an MPC [1]. The signature of these excitations can be seen in the linear transmission spectrum shown in Fig. 2(a).

Nonlinear-optical effects in MPCs were studied by measuring the transmitted SHG intensity $I_{2\omega}$. A Ti:sapphire laser with a 100 fs pulse duration, 80 MHz repetition rate, and 50 mW average power was used as a source of the fundamental beam directed on the MPC from the GGG side, as shown in Fig. 1. The beam was focused on the sample onto a 50 μm diam spot. The second harmonic (SH) generated by the MPC structure was spectrally selected by a set of colored filters and a monochromator and detected by a photomultiplier working in the photon-counting mode. As the fundamental wavelength was tuned in the range from 750 to 860 nm, the corresponding SH wavelengths were far from the MPC resonance region. Both the fundamental and SH waves were p polarized.

The experimental two-dimensional (2D) angular-wavelength SHG intensity spectrum is shown in Fig. 2(b). It exhibits several peculiarities and its spectral position correlates well with the linear transmission results. First, a strong SHG enhancement in the vicinity of Au/air SPP (I) and of several waveguide modes (IIa–IIc) is observed. Second, there is a wide asymmetric modulation of the SHG intensity, which follows the Au/BIG SPP spectral position (III). This modulation is attributed to the SPP excitation on the magnetic Au/BIG interface, as one can clearly see from the comparison with the linear spectra shown in Fig. 2(a). It is important that the spectral positions of the SHG maxima correspond to the WG and air/Au SPP resonances at the fundamental wavelength and should be associated with

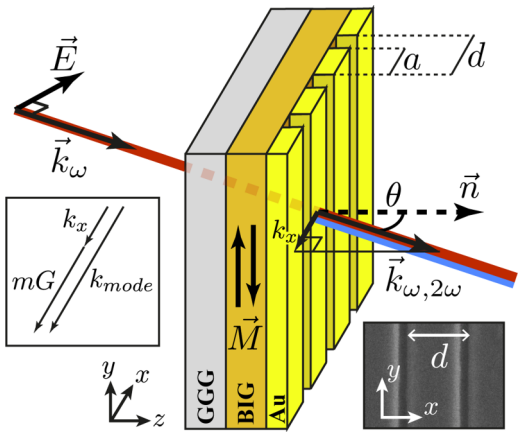

FIG. 1. (Color online) Scheme of the MPC consisting of a magnetic garnet layer on a GGG substrate with a 1D perforated gold structure. A dc magnetic field is applied parallel to the stripes. Insets: Vector diagram for the SHG quasi-phase-matching condition (left) and SEM image of the top view of the sample (right).

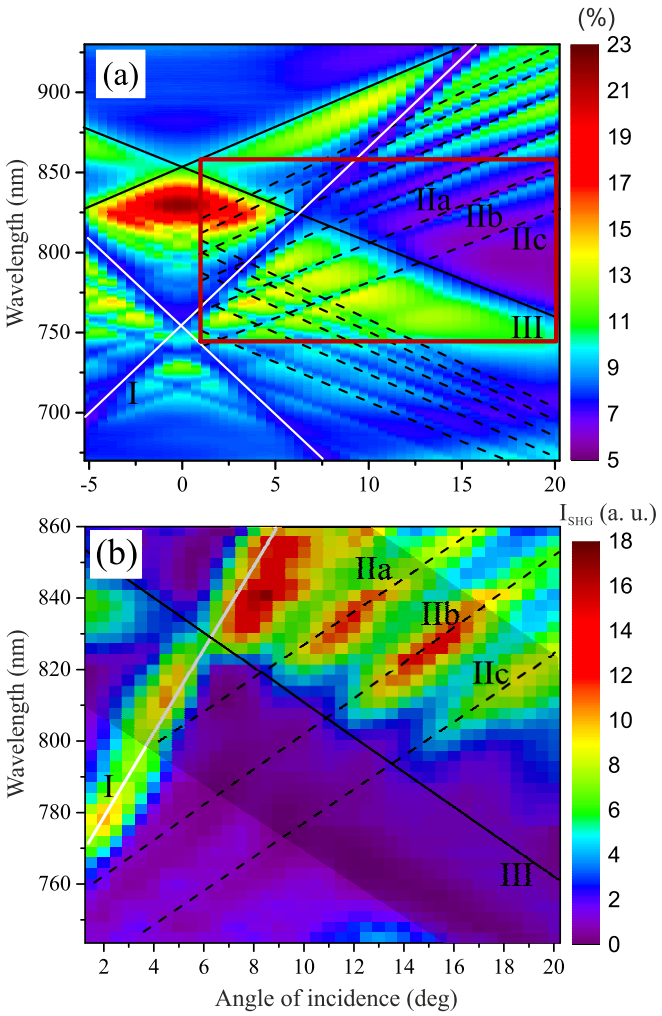

FIG. 2. (Color online) Angular-wavelength spectra of (a) transmission and (b) SHG intensity in a 1D MPC; the y axis corresponds to the fundamental wavelength. The lines indicate the calculated SPP (solid lines) and WG mode (dashed lines) dispersion curves calculated according to Ref. [1]. The darkened area marks the region of intensity modulation caused by the SPP on the Au/BIG interface.

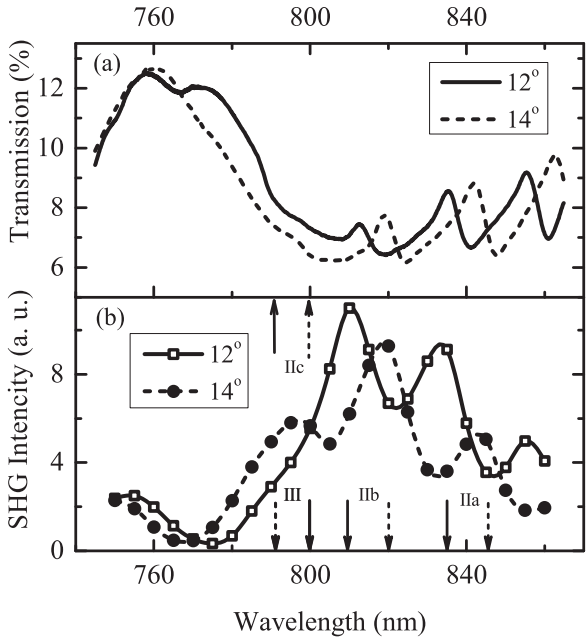

FIG. 3. (a) Transmission and (b) SHG intensity spectra of MPC measured for $\theta = 12^\circ$ and $\theta = 14^\circ$. The arrows show the position of theoretic lines from Fig. 2—solid for 12° and dashed for 14°.

the optical local field amplification. Thus linear and SHG intensity transmission spectra are "inverted," so that the linear transmission minima correspond to increased SHG intensity, as is discussed below.

A strong correlation between the linear and SHG spectra can be seen more explicitly in Fig. 3, which shows such spectra for the two angles of incidence $\theta = 12^\circ, 14^\circ$. It is worth noting that the SHG intensity modulation induced by the excitation of the corresponding resonant modes is dozens of percent, while in the linear case it is at least one order of magnitude lower. A strong redshift of linear and SHG spectra is attained as the θ angle increases, the specific tuning being approximately 5 nm/deg. This tunability is very attractive for potential applications of the MPC structures.

The nonlinear magneto-optical effect was studied as the transversal magnetic field was applied to the MPC. In this case the magnetization-induced SHG intensity modulation can be described by the SHG magnetic contrast, $\rho_{2\omega} = \frac{I_{2\omega}(M) - I_{2\omega}(-M)}{I_{2\omega}(M) + I_{2\omega}(-M)}$, where $I_{2\omega}(\pm M)$ is the SHG intensity measured for the opposite directions of magnetization **M**. The mechanisms underlying the magnetic-field-induced SHG effects were first discussed in detail in Ref. [19]. In brief, the SHG intensity may be expressed as $I_{2\omega} \propto \left| P_{2\omega}^{\text{cryst}} e^{i\Phi_{2\omega}^{\text{cryst}}} + P_{2\omega}^{M} e^{i\Phi_{2\omega}^{M}} \right|^2$, where $P_{2\omega}^{\text{cryst}}, P_{2\omega}^{M}$ and $\Phi_{2\omega}^{\text{cryst}}, \Phi_{2\omega}^{M}$ are the amplitudes and phases of the so-called crystallographic and magnetization-induced SHG terms, respectively. Close to the resonant excitation of SPP or WG modes one would expect a different spectral behavior of these parameters, while the SHG contrast is always determined by both the amplitudes and the relative phase of these two contributions [20],

$$\rho_{2\omega} \approx 2 \left| P_{2\omega}^{M} \right| \Big/ \left| P_{2\omega}^{\text{cryst}} \right| \cos\left(\Phi_{2\omega}^{M} - \Phi_{2\omega}^{\text{cryst}} \right). \qquad (1)$$

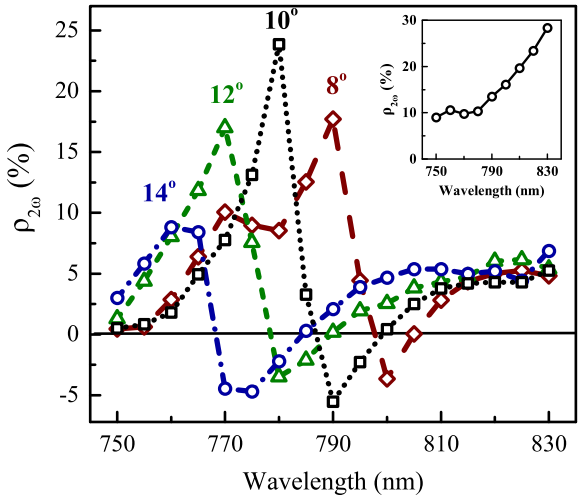

FIG. 4. (Color online) SHG magnetic contrast vs the fundamental wavelength measured for $\theta = 8°$, $10°$, $12°$, and $14°$. The inset shows the $\rho_{2\omega}$ spectrum measured for the bare BIG film.

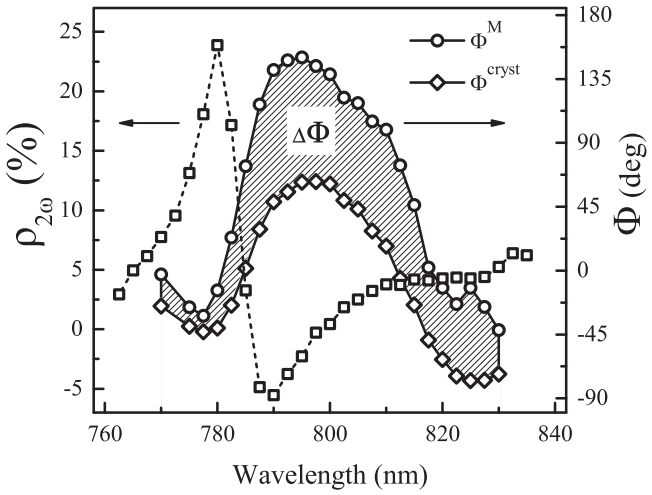

FIG. 5. Spectra of the SHG magnetic contrast (left scale) and phases of the magnetization-dependent Φ^M and independent Φ^{cryst} second harmonic components (right scale). $\theta = 10°$.

Figure 4 shows $\rho_{2\omega}$ spectra obtained for various θ values. It can be seen that the SHG magnetic contrast has a strong peculiarity in the vicinity of Au/BIG SPP excitation. Within this spectral range, $\rho_{2\omega}$ exhibits two features, namely, an increase of the absolute $\rho_{2\omega}$ value up to 24% and the change of the sign of the SHG contrast. Also, it should be pointed out that the WG modes contribute much less to the $\rho_{2\omega}$ spectrum, as there are no strong peculiarities at the corresponding wavelengths in this spectrum.

The inset in Fig. 4 shows the SHG magnetic contrast spectrum measured for a reference homogeneous bare garnet film; it reveals a monotonous $\rho_{2\omega}$ spectral growth up to a value of 30% for a fundamental wavelength of 830 nm. At the same time, it does not demonstrate any type of resonant behavior or a change in the $\rho_{2\omega}$ sign as in the case of the MPC structure.

For a full characterization of the magnetic-field-induced effects in the MPC nonlinear response, SHG phase measurements were performed. We used a one-beam SH interferometry technique [21] with a thin indium tin oxide (ITO) film used as a reference SHG source that was placed on a translation stage after the sample. The phase of the SHG magnetic component was obtained by measuring the phases of the SHG waves generated for the opposite directions of the applied magnetic field [20]. Following the procedure described in Ref. [20], the spectral dependencies of the SHG field components induced by $P_{2\omega}^{\text{cryst}}$ and $P_{2\omega}^{M}$ were determined. Figure 5 shows the corresponding SHG phase spectra for $\theta = 10°$. It can be seen that the nonmagnetic SHG phase $\Phi_{2\omega}^{\text{cryst}}$ within the Au/BIG SPP excitation area ($\sim$ 770–830 nm) experiences a change on approximately 130°, while the $\Phi_{2\omega}^{M}$ variation exceeds 180°. Such a nonuniform phase behavior may be attributed to the asymmetric (Fano) shape of the resonance. Thus we see that the phase difference $\Delta\Phi = \Phi_{2\omega}^{M} - \Phi_{2\omega}^{\text{cryst}}$ reaches a value of more than 90° near the resonance, which changes the sign of the SHG magnetic contrast.

Though the linear-optical effects in similar MPCs are well studied [1–6], for the nonlinear response the picture is much less clear. First of all, the SHG being an even-order nonlinear process is prohibited in the electric dipole approximation in the bulk of centrosymmetric media (such as BIG, Au, and GGG). This means that the SHG in magnetoplasmonic crystals is formed predominantly by contributions from the interfaces: air/Au, Au/BIG, BIG/GGG, and GGG/air. The SH generated on the latter two ones is absorbed in the BIG layer and does not contribute to the detected SHG. The SHG intensity is given by [22] $I_{2\omega} \propto |\mathbf{P}_{2\omega}|^2 \propto |\hat{\chi}^{(2)}\vdots\mathbf{E}_{\omega}\mathbf{E}_{\omega}|^2$, where $\mathbf{P}_{2\omega}$ is the complex polarization at 2ω, $\hat{\chi}^{(2)}$ is the nonlinear susceptibility tensor, and $\mathbf{E}_{\omega}$ is the *local* fundamental field amplitude.

It is worth noting that due to a complicated MPC structure, the SHG response is typically determined by an interference of various SH contributions that can be excited at MPC interfaces and that can have different resonant features. If so, a *nonlinear* Fano-type resonance should give an asymmetric shape of the SHG intensity maxima, similarly to that shown in Fig. 3(b).

Magnetization leads to additional symmetry properties of the surface and thus may influence both the fundamental local field $\mathbf{E}_{\omega}$ and the nonlinear polarization $\mathbf{P}_{2\omega}$ as well. In the case of MPCs, the modification of the fundamental field is regarded as the result of the magnetic-field-induced spectral shift of the MPC resonances observed previously [1] and leading to the transversal magneto-optical effect. This magneto-induced spectral shift is up to $\sim$0.1 nm (for a saturating magnetic field) and should lead to the same magneto-induced shift of the SHG intensity spectrum, due to the nonresonant nature of $\chi^{(2)}$ itself. Using the experimentally measured SHG intensity spectrum, we can estimate the maximum value of the corresponding magneto-induced SHG intensity change as $\sim$1% (for the 12° incidence angle), which is much smaller than the one observed in the experiment. This encourages us to search for another mechanism of the magnetic-field-induced effects in SHG.

Magnetization-induced modifications of the nonlinear susceptibility are described by the *odd* with respect to the magnetization (magnetization-induced, denoted below by the superscript M) components of the susceptibility tensor $\chi^{(2)M}$. Their symmetry differs from that of the nonmagnetic (crystallographic) components $\hat{\chi}^{(2)\text{cryst}}$, thus giving rise to the

nonlinear magneto-optical polarization and intensity effects that are linear in magnetization [19]. The second harmonic in the vicinity of the Au/BIG SPP excitation consists of two contributions: the resonant contribution from the magnetic Au/BIG interface and a nonresonant and nonmagnetic SH, generated at the Au/air interface. The first contribution leads to resonant spectral dependencies of both the magnetic and crystallographic parts.

The observed strongly resonant behavior of the SHG contrast $\rho_{2\omega}$, given by Eq. (1), and especially its sign inversion close to the Au/BIG SPP resonant excitation, is a clear evidence of drastic spectral changes of the relative phase $\Delta\Phi = \Phi_{2\omega}^{\text{cryst}} - \Phi_{2\omega}^{M}$. This requires different spectral dependencies of the magnetic and nonmagnetic SHG contributions, which may occur due to different mechanisms that give rise to these parts of the SH. An important point here is that only the nonmagnetic SHG component has a nonresonant part due to the contribution of the Au/air interface in the SHG signal, which leads to a decrease of the spectral modulation of the absolute amplitude and the phase $\Phi_{2\omega}^{\text{cryst}}$ of this term. This results in a stronger phase shift of the magnetic contribution, compared to the nonmagnetic one, and in an increase of the absolute $\rho_{2\omega}$ value observed in the vicinity of Au/BIG SPP excitation.

Another mechanism which can affect the resonant enhancement of $\rho_{2\omega}$ is related to the interplay between different $\hat{\chi}^{(2)\text{cryst}}$ and $\hat{\chi}^{(2)M}$ susceptibility components, which have different symmetry properties. To illustrate this idea we assume that two components, $\hat{\chi}_{zzz}^{(2)\text{cryst}}$ and $\hat{\chi}_{xxx}^{(2)M}$, give the main contribution to the p-polarized SHG. The corresponding SHG fields are induced by the local field components E_x and E_z. In general, close to the resonant SPP excitation, the corresponding enhancement factors $L_x \neq L_z$, because the electric field of the SPP wave is predominantly transversal. Thus the spectral enhancement of the magnetic and of the nonmagnetic SHG terms is different (given by $L_x^2 \neq L_z^2$, respectively), which affects the spectral dependence of the SHG magnetic contrast.

In summary, we have demonstrated results of optical second harmonic generation in a 1D Au/BIG magnetoplasmonic crystal. The structure supports excitation of several resonant electromagnetic modes, which affects both the linear- and nonlinear-optical response. Particularly, the SHG intensity exhibits a strong enhancement due to the optical field localization in the SPP or waveguide modes. The nonuniform field distribution and enhancement in the presence of the SPP on the Au/BIG interface leads to different spectral dependencies of the magneto-induced and nonmagnetic components of the SH signal. This difference provides an enhancement of the SHG intensity contrast up to 25%, which follows the resonance position on the dispersion curve. The coexistence of spectral regions with simultaneous enhancement of the SHG intensity and magnetic contrast makes the considered MPC structure promising as an effective tunable nonlinear-optical photonic element.

Financial support by RFBR Grant No. 13-02-01102 is acknowledged.

[1] A. Chekhov, V. Krutyanskiy, A. Shaimanov, A. Stognij, and T. Murzina, Opt. Express **22**, 17762 (2014).
[2] A. A. Grunin, A. G. Zhdanov, A. A. Ezhov, E. A. Ganshina, and A. A. Fedyanin, Appl. Phys. Lett. **97**, 261908 (2010).
[3] V. I. Belotelov, I. A. Akimov, M. Pohl, V. A. Kotov, S. Kasture, A. S. Vengurlekar, A. V. Gopal, D. R. Yakovlev, A. K. Zvezdin, and M. Bayer, Nat. Nanotechnol. **6**, 370 (2011).
[4] V. I. Belotelov, L. E. Kreilkamp, I. A. Akimov, A. N. Kalish, D. A. Bykov, S. Kasture, V. J. Yallapragada, A. V. Gopal, A. M. Grishin, S. I. Khartsev, M. Nur-E-Alam, M. Vasiliev, L. L. Doskolovich, D. R. Yakovlev, K. Alameh, A. K. Zvezdin, and M. Bayer, Nat. Commun. **4**, 2128 (2013).
[5] M. Pohl, L. E. Kreilkamp, V. I. Belotelov, I. A. Akimov, A. N. Kalish, N. E. Khokhlov, V. J. Yallapragada, A. V. Gopal, M. Nur-E-Alam, M. Vasiliev, D. R. Yakovlev, K. Alameh, A. K. Zvezdin, and M. Bayer, New J. Phys. **15**, 075024 (2013).
[6] G. Armelles, A. Cebollada, A. Garcia-Martin, J. M. Garcia-Martin, M. U. Gonzalez, J. B. Gonzalez-Diaz, E. Ferreiro-Vila, and J. F. Torrado, J. Opt. A: Pure Appl. Opt. **11**, 114023 (2009).
[7] V. I. Belotelov, I. A. Akimov, M. Pohl, A. N. Kalish, S. Kasture, A. S. Vengurlekar, A. V. Gopal, V. A. Kotov, D. Yakovlev, A. K. Zvezdin, and M. Bayer, J. Phys.: Conf. Ser. **303**, 012038 (2011).
[8] M. Futamata, J. Phys. Chem. **99**, 11901 (1995).
[9] H. J. Simon, D. E. Michell, and J. G. Watson, Phys. Rev. Lett. **33**, 1531 (1974).
[10] J. L. Coutaz, M. Neviere, E. Pic, and R. Reinisch, Phys. Rev. B **32**, 2227 (1985).
[11] Y. R. Shen, Nature (London) **337**, 519 (1989).
[12] V. L. Krutyanskiy, I. A. Kolmychek, E. A. Gan'shina, T. V. Murzina, P. Evans, R. Pollard, A. A. Stashkevich, G. A. Wurtz, and A. V. Zayats, Phys. Rev. B **87**, 035116 (2013).
[13] G. Tessier, C. Malouin, P. Georges, A. Brun, D. Renard, V. V. Pavlov, P. Meyer, J. Ferré, and P. Beauvillain, Appl. Phys. B **68**, 545 (1999).
[14] W. Zheng, A. T. Hanbicki, B. T. Jonker, and G. Lüpke, Opt. Express **21**, 28842 (2013).
[15] D. M. Newman, M. I. Wears, R. J. Matelon, and D. McHugh, Appl. Phys. B **74**, 719 (2002).
[16] I. Razdolski, D. G. Gheorghe, E. Melander, B. Hjorvarsson, P. Patoka, A. V. Kimel, A. Kirilyuk, E. T. Papaioannou, and T. Rasing, Phys. Rev. B **88**, 075436 (2013).
[17] A. V. Bespalova, O. L. Golikovaa, S. S. Savina, A. I. Stognij, and N. N. Novitskiib, Inorg. Mater. **48**, 1190 (2012).
[18] M. Pashkevich, R. Gieniusz, A. Stognij, N. Novitskii, A. Maziewski, and A. Stupakiewicz, Thin Solid Films **556**, 464 (2014).
[19] R.-P. Pan, H. D. Wei, and Y. R. Shen, Phys. Rev. B **39**, 1229 (1989).
[20] T. V. Murzina, I. A. Kolmychek, A. A. Nikulin, E. A. Gan'shina, and O. A. Aktsipetrov, JETP Lett. **90**, 504 (2009).
[21] K. Kemnitz, K. Bhattacharyya, J. M. Hicks, G. R. Pinto, B. Eisenthal, and T. F. Heinz, Chem. Phys. Lett. **131**, 285 (1986).
[22] Y. R. Shen, *The Principles of Nonlinear Optics* (Wiley-Interscience, New York, 1984).